Quarkonium Production in the Color Evaporation Model

R. Vogt

Nuclear Science Division, Lawrence Berkeley National Laboratory, Berkeley, CA 94720, USA
and
Physics Department, University of California, Davis, CA 95616, USA

J/ψ Production is a 'Hard' Process

'Hard' processes have a large scale in the calculation that makes perturbative QCD applicable: high momentum transfer, Q^2, high invariant mass, M, high transverse momentum, p_T

Assumption of asymptotic freedom allows calculation of hard processes on the partonic level

Confinement constrains partons to hadrons

Factorization between the perturbative hard part and the universal, nonperturbative parton distribution functions allows calculation

$$\begin{aligned}\sigma_{AB}(s, m_Q^2) &= \sum_{i,j=q,\overline{q},g} \int_{4m_Q^2/s}^{1} \frac{d\tau}{\tau} \int dx_1\, dx_2\, \delta(x_1 x_2 - \tau) \\ &\quad \times f_{i/A}(x_1, \mu^2)\, f_{j/B}(x_2, \mu^2)\, \widehat{\sigma}_{ij}(\tau, m_Q^2, \mu^2)\end{aligned}$$

$f_{i/A}$ are the parton distributions, either in a proton or a nucleus, determined from fits to data, x_1 and x_2 are the fractional momentum of the hadron carried by partons i and j

$\widehat{\sigma}_{ij}(\tau, m_Q^2, \mu^2)$ is partonic cross section calculable in QCD in powers of α_s^{2+n}: LO, $n = 0$; NLO, $n = 1$ ...

Quarkonium Production in the Color Evaporation Model (CEM)

Gavai *et al.*, G. Schuler and R.V.

All quarkonium states are treated like $Q\overline{Q}$ ($Q = c, b$) below $H\overline{H}$ ($H = D, B$) threshold

Distributions for all charmonium family members identical. Thus production ratios should also be identical with $\sqrt{S}$, p_T, x_F.

At LO, $gg \to Q\overline{Q}$ and $q\overline{q} \to Q\overline{Q}$; NLO add $gq \to Q\overline{Q}q$

$$\sigma_Q^{\rm CEM} = F_Q \sum_{i,j} \int_{4m_Q^2}^{4m_H^2} d\hat{s} \int dx_1 dx_2 \; f_{i/p}(x_1, \mu^2) \; f_{j/p}(x_2, \mu^2) \; \hat{\sigma}_{ij}(\hat{s}) \; \delta(\hat{s} - x_1 x_2 s)$$

First, values of m_Q and Q^2 for several parton densities fixed from NLO calculation of $Q\overline{Q}$ total cross sections

Inclusive F_Q fixed by comparison of NLO calculation of $\sigma_Q^{\rm CEM}$ to $\sqrt{S}$ dependence of J/ψ and Υ cross sections, $\sigma(x_F > 0)$ and $B d\sigma/dy|_{y=0}$ for J/ψ, $B d\sigma/dy|_{y=0}$ for Υ

Data and branching ratios used to separate the F_Q's for each quarkonium state

$\chi_c/J/\psi$ Ratio Energy Independent

HERA-B plot comparing $R_{\chi_c} = \sigma(\chi_c)/\sigma(J/\psi)$ with πA and pA data

Result is most consistent with R_{χ_c} independent of $\sqrt{S}$, as predicted by CEM

CDF result, $R_{\chi_c} = 0.297 \pm 0.017 \pm 0.057$, consistent with fixed-target results

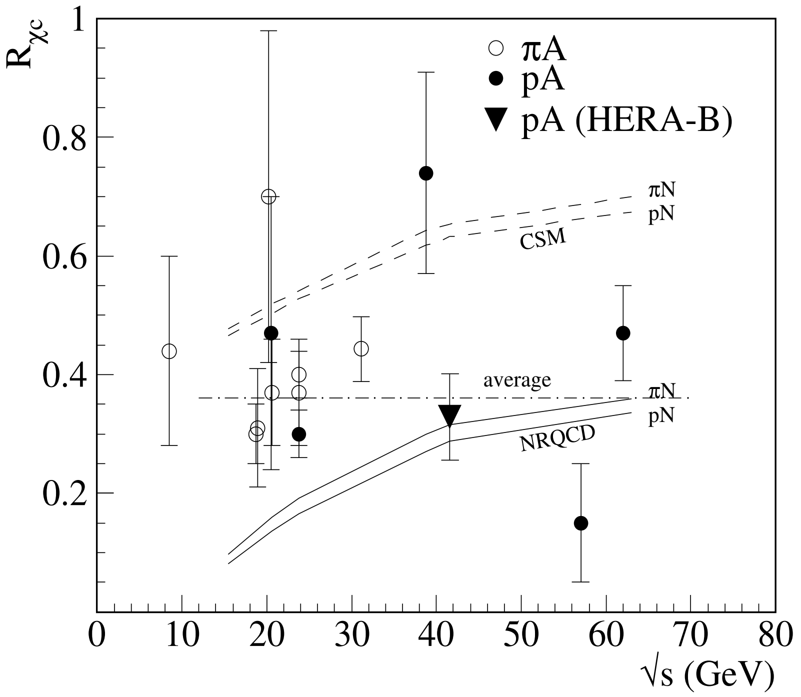

Figure 1: Ratio of χ_c to J/ψ cross sections as a function of $\sqrt{S}$ for πA and pA fixed-target measurements. The CSM and NRQCD curves are obtained from Monte Carlo while the 'average' is the average value of all measurements. From I. Abt *et al.* (HERA-B Collab.), Phys. Lett. **561** (2003) 61.

$\psi'/J/\psi$ Ratio Also Energy Independent

Data are from pp and pA interactions

Solid curve corresponds to CEM

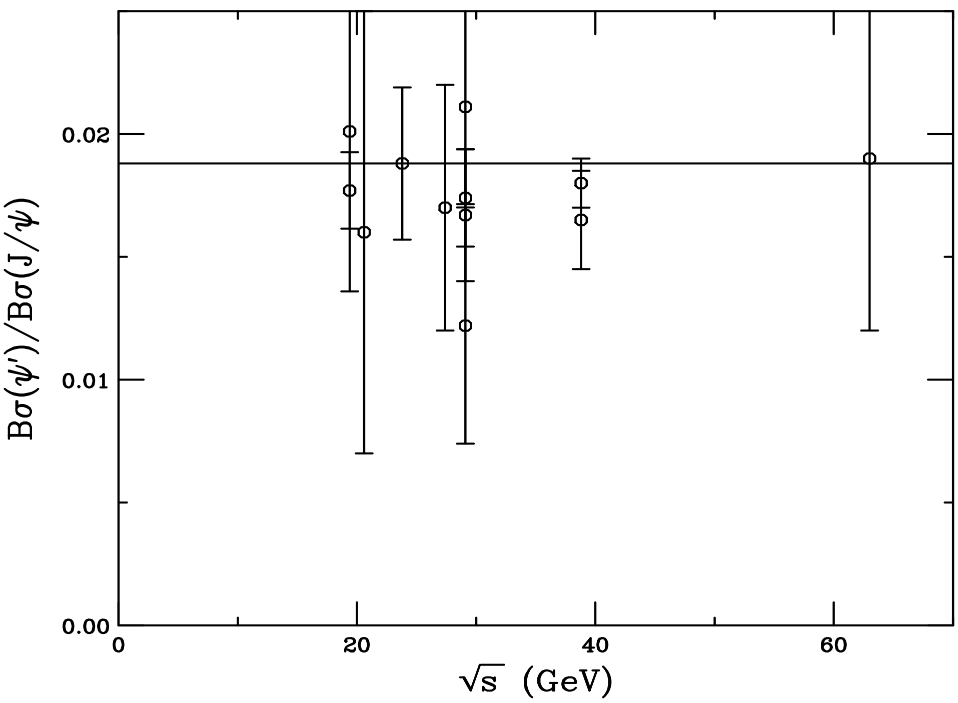

Figure 2: Ratio of ψ' to J/ψ cross sections with lepton pair branching ratios included as a function of $\sqrt{S}$ for pp and pA measurements. Adapted from R.V., Phys. Rept. **310** (1999) 197.

Production and Feeddown Fractions

Resonance	$\sigma_i^{\rm dir}/\sigma_H$	f_i
J/ψ	0.62	0.62
ψ'	0.14	0.08
χ_{c1}	0.6	0.16
χ_{c2}	0.99	0.14
Υ	0.52	0.52
Υ'	0.33	0.10
Υ''	0.20	0.02
$\chi_b(1P)$	1.08	0.26
$\chi_b(2P)$	0.84	0.10

Table 1: The ratios of the direct quarkonium production cross sections, $\sigma_i^{\rm dir}$, to the inclusive J/ψ and Υ cross sections, denoted σ_H, and the feeddown contributions of all states to the J/ψ and Υ cross sections, f_i.

$c\overline{c}$ Data Fixes Mass and Scale for CEM Charmonium Calculations

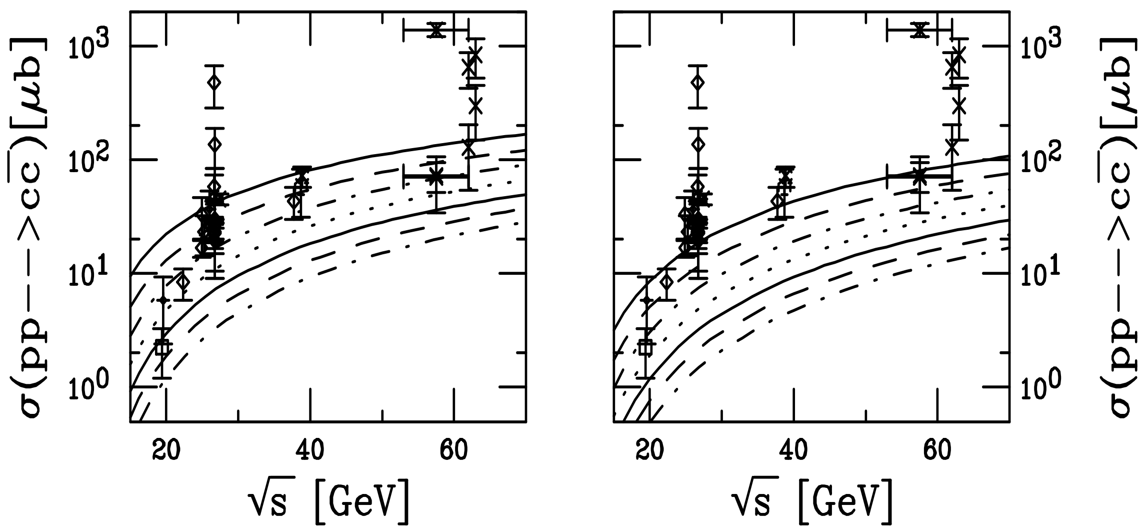

Figure 3: Total $c\overline{c}$ cross sections in pp interactions as a function of m_c. These NLO calculations use the MRST HO parton densities. The left-hand plot shows the results with $\mu_F = \mu_R = \mu = m_c$ while in the right-hand plot, $\mu = 2m_c$. From top to bottom the curves are $m_c = 1.2$, 1.3, 1.4, 1.5, 1.6, 1.7, and 1.8 GeV.

Parameters From $c\bar{c}$ Cross Sections

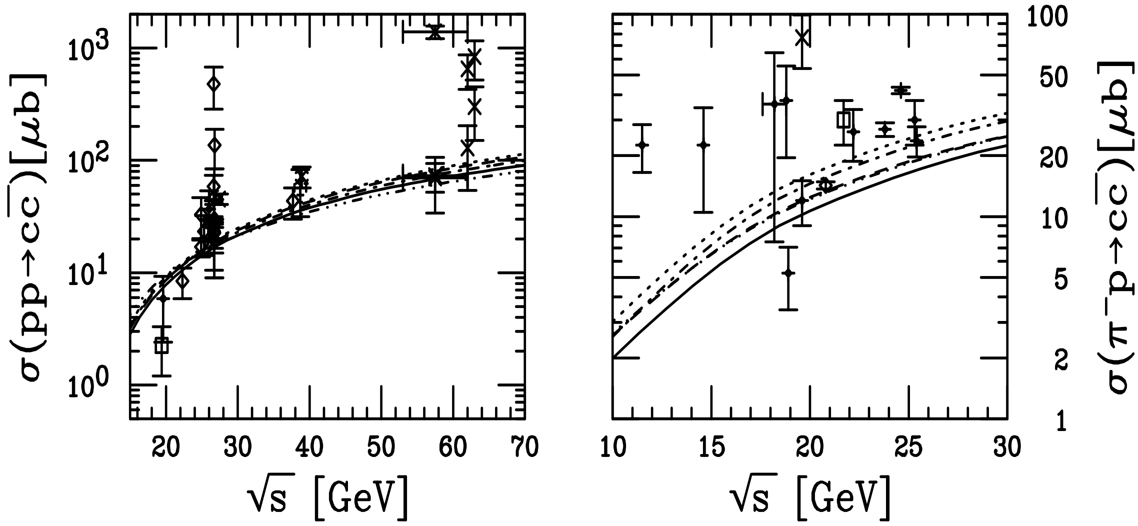

Figure 4: Total $c\bar{c}$ cross sections in pp and $\pi^- p$ interactions. The curves are: MRST HO with $\mu = m = 1.4$ GeV (solid) and $\mu = 2m = 2.4$ GeV (dashed); CTEQ 5M with $\mu = m = 1.4$ GeV (dot-dashed) and $\mu = 2m = 2.4$ GeV (dotted); and GRV 98 HO with $\mu = m = 1.3$ GeV.

Case	PDF	m_c (GeV)	μ/m_c	$\sigma_{J/\psi}/\sigma_C^{\rm CEM}$
$\psi1$	MRST HO	1.2	2	0.0144
$\psi2$	MRST HO	1.4	1	0.0248
$\psi3$	CTEQ 5M	1.2	2	0.0155
$\psi4$	GRV 98 HO	1.3	1	0.0229

Table 2: The production fractions obtained from fitting the CEM cross section to the J/ψ total cross sections and $y = 0$ cross sections as a function of energy. The PDF, charm quark mass, and scales used are the same as those obtained by comparison of the $c\bar{c}$ cross section to the pp data.

J/ψ Production Cross Sections vs. Forward Data

Forward J/ψ cross sections compared to data

Inclusive J/ψ cross section–all figures include feeddown from χ_c and ψ'

Same parameters used as those that agree with $c\overline{c}$ total cross sections

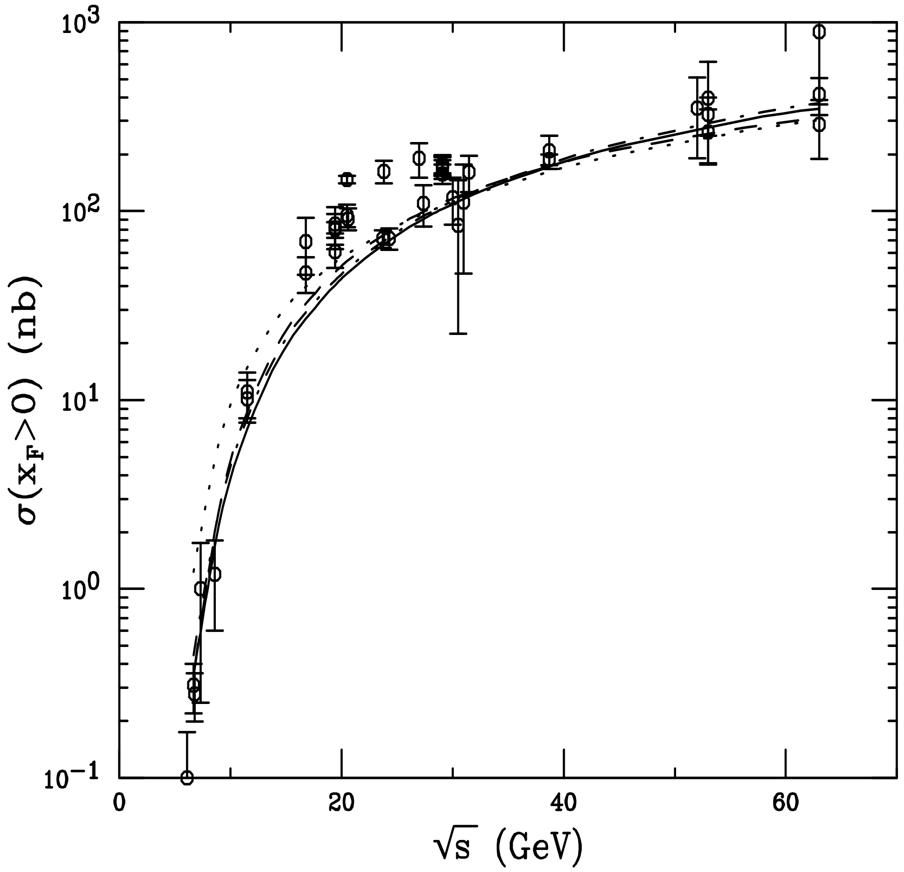

Figure 5: J/ψ production data on total cross sections with $x_F > 0$ compared to NLO CEM calculations. The solid curve employs the MRST HO distributions with $m_c = \mu/2 = 1.2$ GeV, the dashed, MRST HO with $m_c = \mu = 1.4$ GeV, the dot-dashed, CTEQ 5M with $m_c = \mu/2 = 1.2$ GeV, and the dotted, GRV 98 HO with $m_c = \mu = 1.3$ GeV.

J/ψ Production Cross Sections at $y = 0$

Inclusive $J/\psi \to l^+l^-$ cross sections compared to data

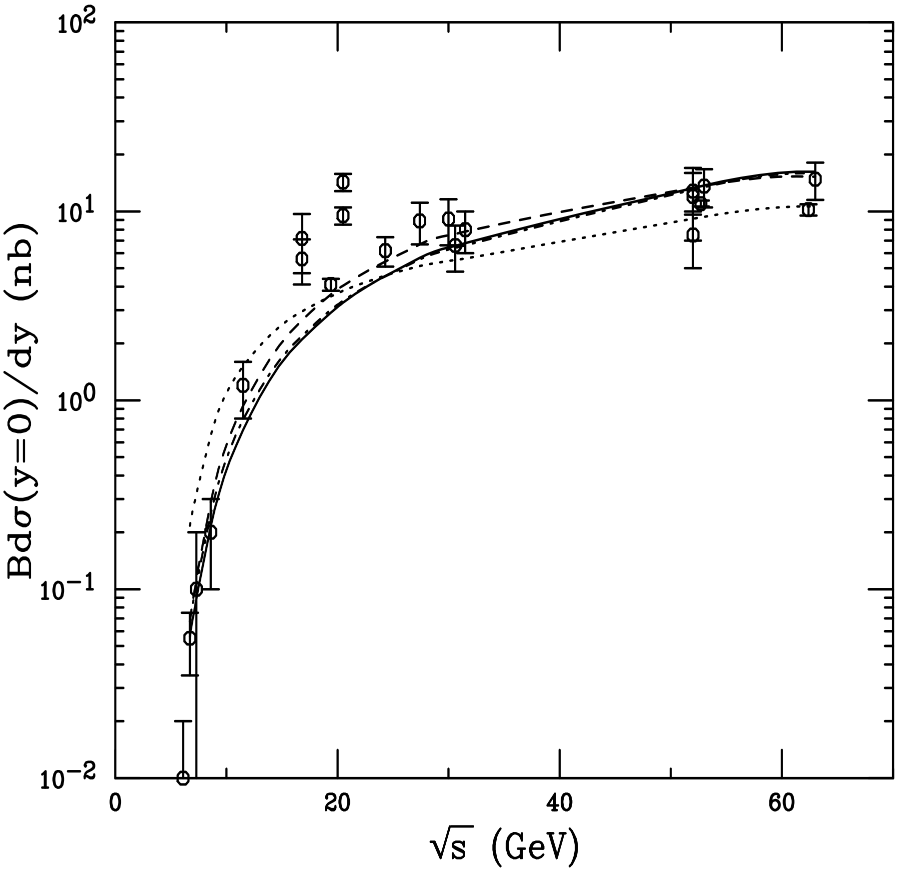

Figure 6: J/ψ production data at $y = 0$ compared to NLO CEM calculations. The solid curve employs the MRST HO distributions with $m_c = \mu/2 = 1.2$ GeV, the dashed, MRST HO with $m_c = \mu = 1.4$ GeV, the dot-dashed, CTEQ 5M with $m_c = \mu/2 = 1.2$ GeV, and the dotted, GRV 98 HO with $m_c = \mu = 1.3$ GeV.

Extrapolated J/ψ Total Cross Sections

Total forward J/ψ cross sections extrapolated to higher energy

Energy dependence obtained from NLO CEM

Factor of $\sim$ 1.6 between results at 200 GeV, similar at 5.5 TeV

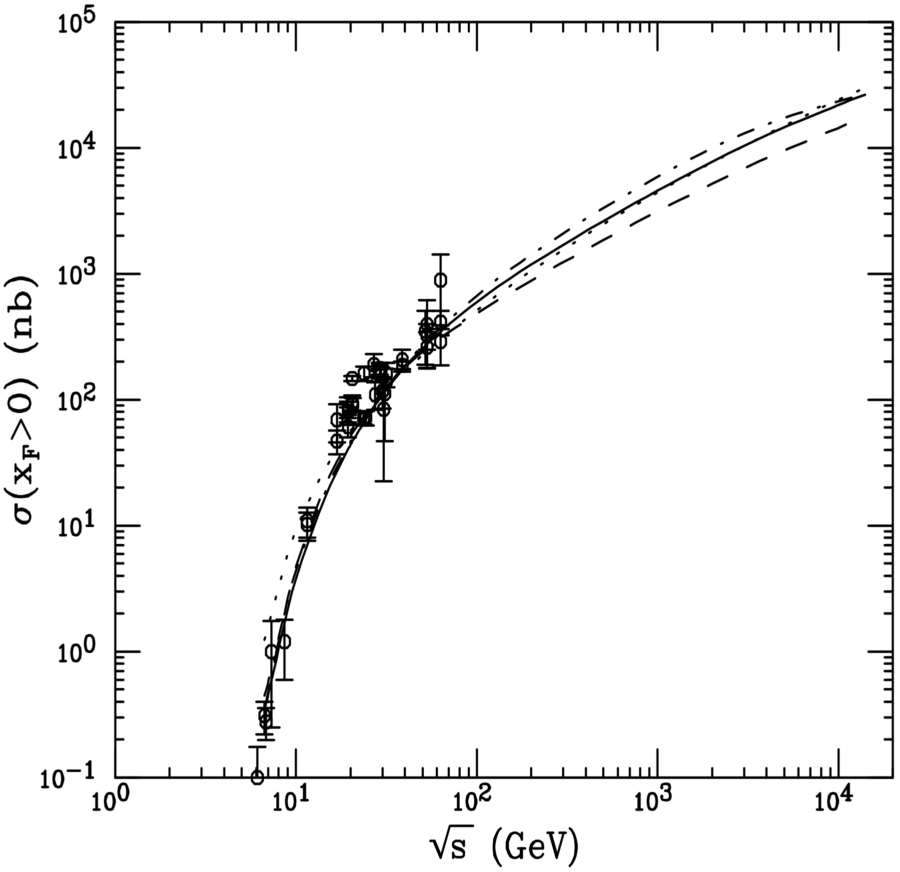

Figure 7: NLO J/ψ forward cross sections. The solid curve employs the MRST HO distributions with $m_c = \mu/2 = 1.2$ GeV, the dashed, MRST HO with $m_c = \mu = 1.4$ GeV, the dot-dashed, CTEQ 5M with $m_c = \mu/2 = 1.2$ GeV, and the dotted, GRV 98 HO with $m_c = \mu = 1.3$ GeV.

CEM Describes J/ψ x_F Distributions Reasonably Well

Hadroproduction data with a variety of beam-target combinations

Normalization agrees rather well with x_F distributions when calculated at NLO

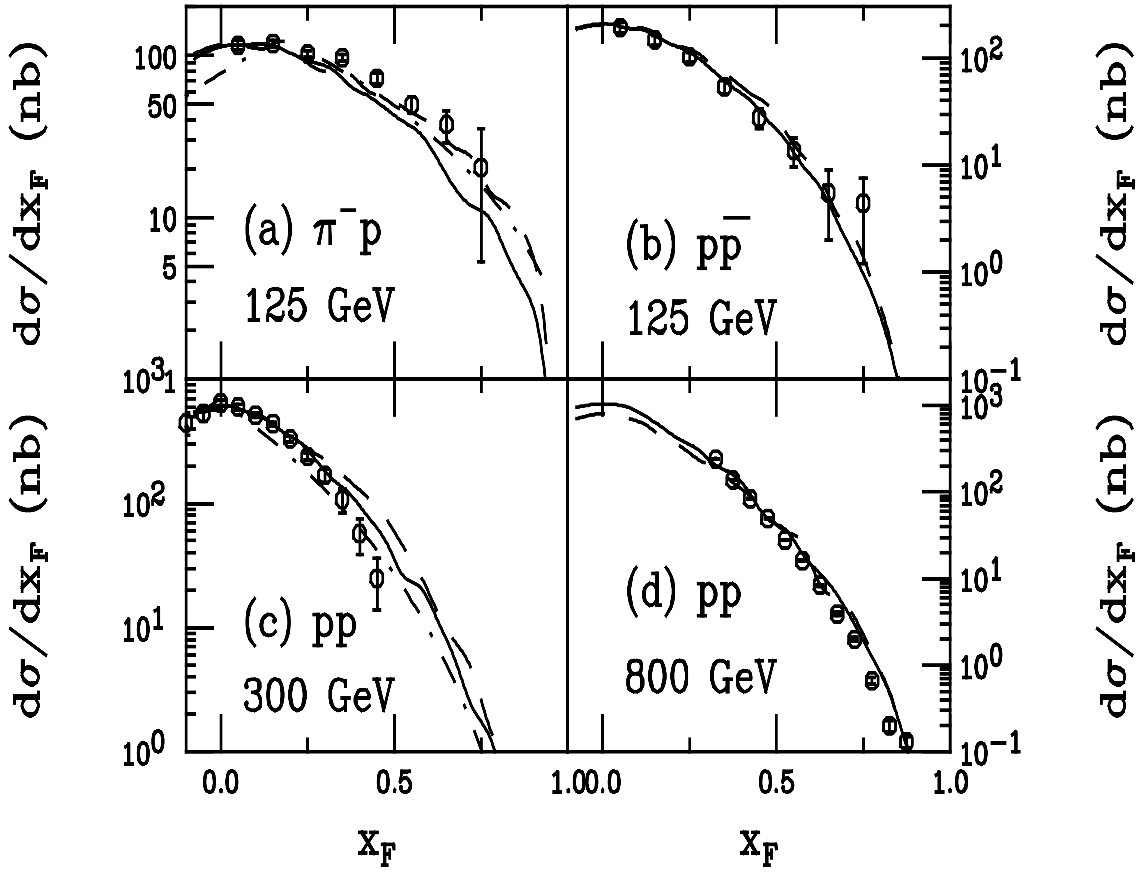

Figure 8: CEM x_F distributions of J/ψ production calculated to NLO. A Be target is used in (a), (b) and (d) while a Li target is used in (c). From R.V., Phys. Rept. **310** (1999) 197.

Comparison to CDF Charmonium Data

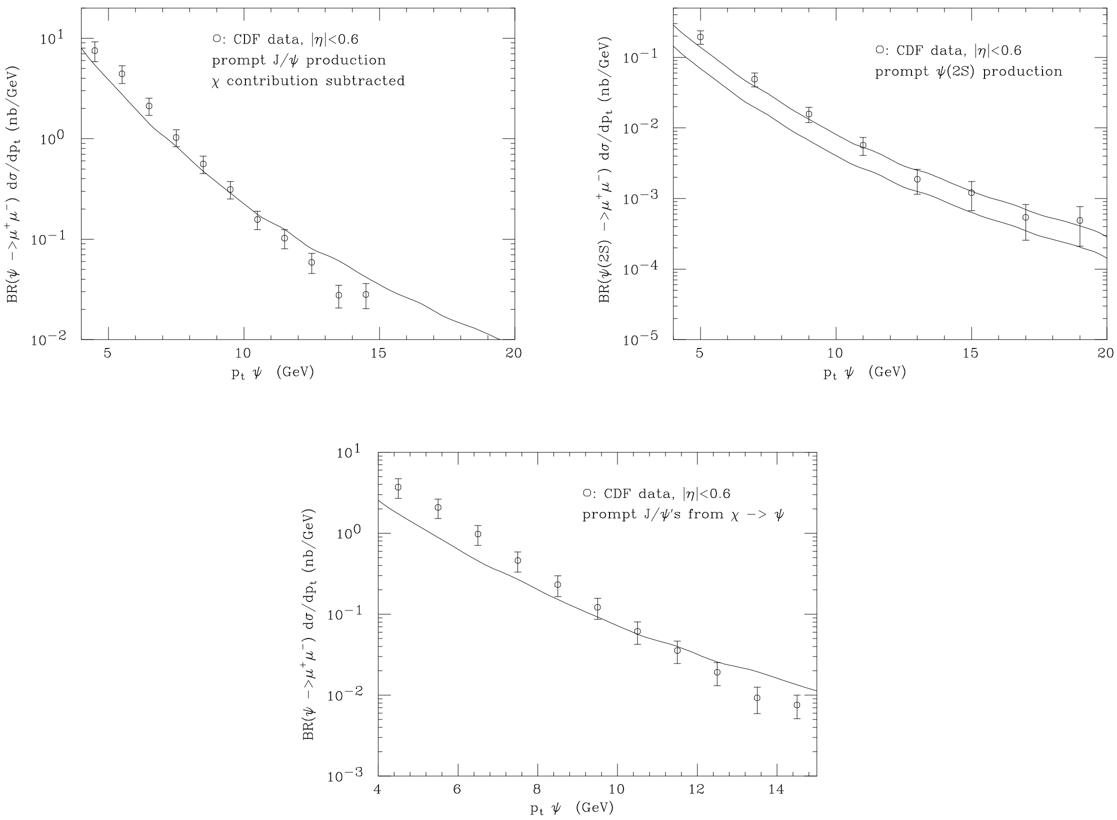

Figure 9: Transverse momentum distributions of charmonia compared to CDF data. The upper curve for $\psi(2S)$ contains a K factor of 2. From G. Schuler and R.V., Phys. Lett. **B387** (1996) 181.

Comparison to PHENIX J/ψ pp Rapidity Data

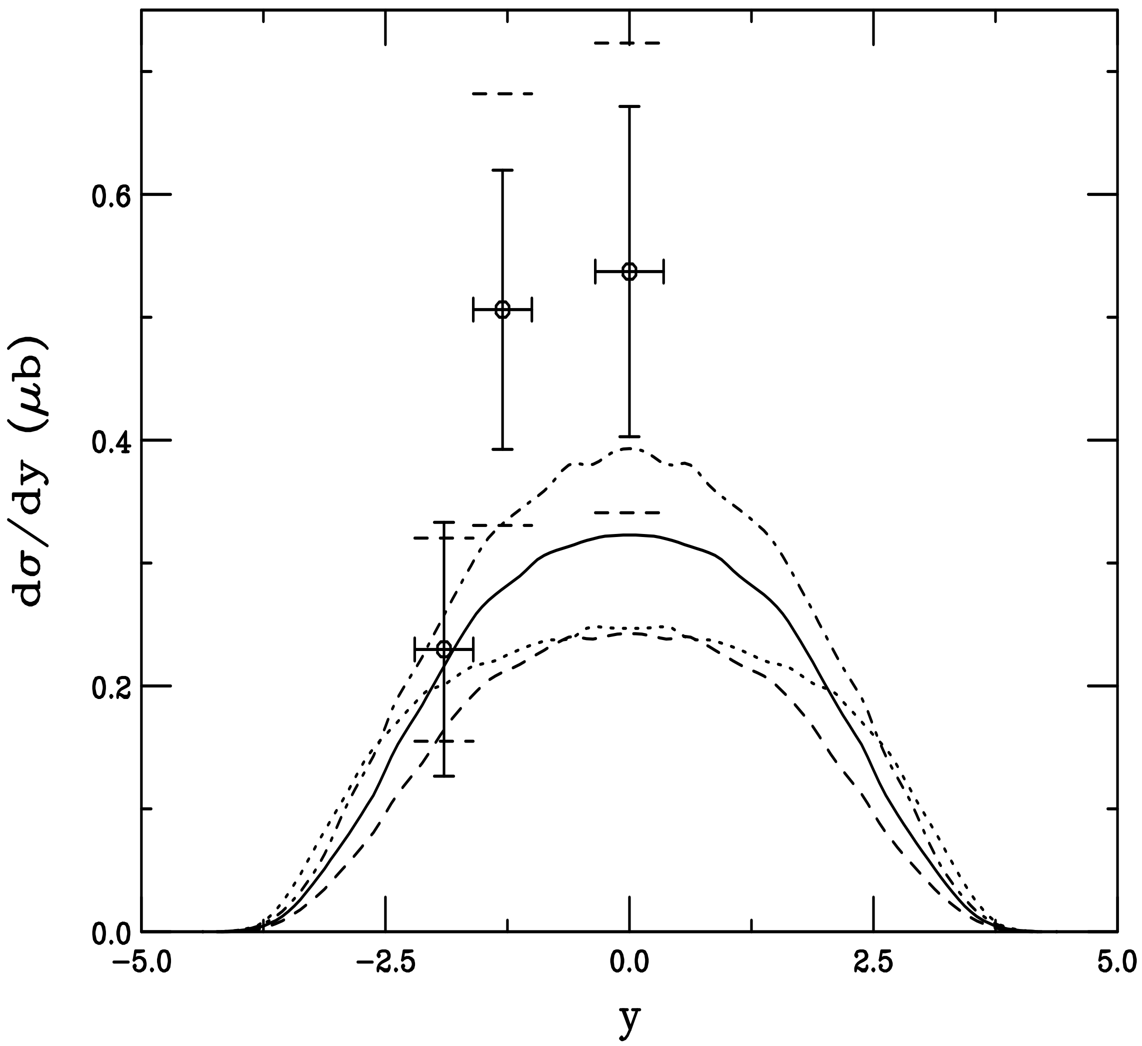

Figure 10: Direct J/ψ rapidity distributions compared to PHENIX data from Quark Matter '02. The data points are scaled to remove the $J/\psi \rightarrow l^+l^-$ branching ratio and to include direct production only. The solid curve employs the MRST HO distributions with $m_c = \mu/2 = 1.2$ GeV, the dashed, MRST HO with $m_c = \mu = 1.4$ GeV, the dot-dashed, CTEQ 5M with $m_c = \mu/2 = 1.2$ GeV, and the dotted, GRV 98 HO with $m_c = \mu = 1.3$ GeV.

Extrapolated J/ψ Cross Sections at $y = 0$

Model cross sections extrapolated to RHIC energies with the preliminary PHENIX e^+e^- point at $y \sim 0$

Also shown is old Craigie parameterization,
$Bd\sigma/dy|_{y=0} = 50\exp(-14.7 m_{J/\psi}/\sqrt{s})$ nb

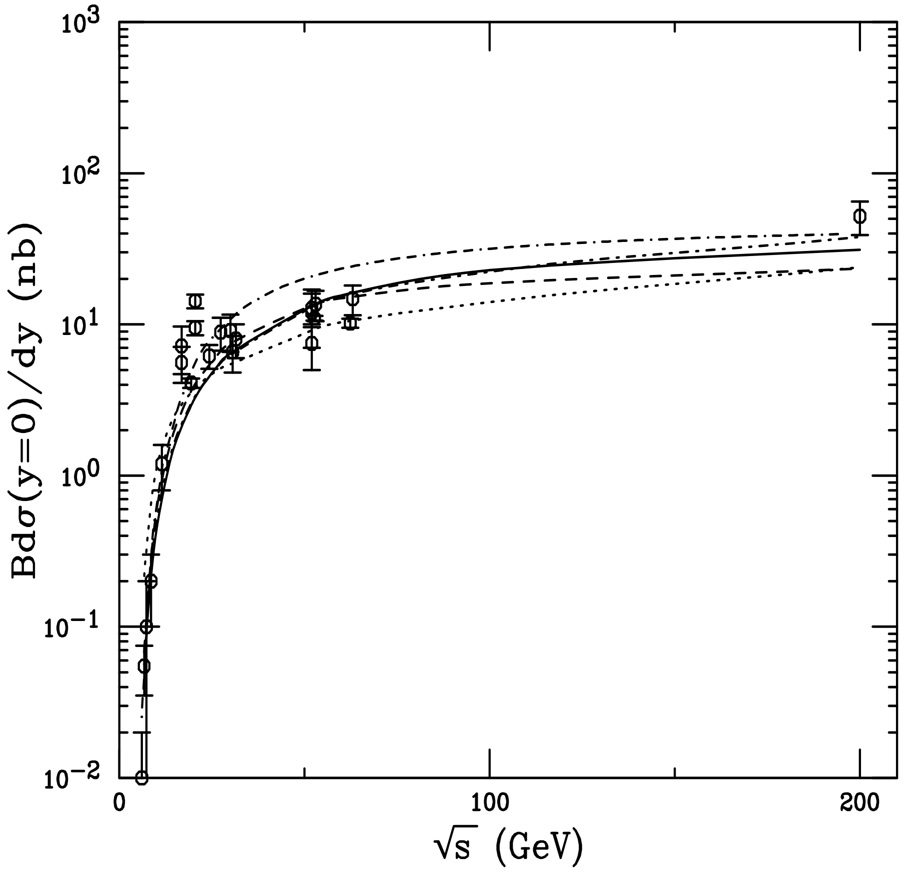

Figure 11: J/ψ production data at $y = 0$ compared to NLO CEM calculations. The solid curve employs the MRST HO distributions with $m_c = \mu/2 = 1.2$ GeV, the dashed, MRST HO with $m_c = \mu = 1.4$ GeV, the dot-dashed, CTEQ 5M with $m_c = \mu/2 = 1.2$ GeV, and the dotted, GRV 98 HO with $m_c = \mu = 1.3$ GeV. The dot-dash-dash-dashed curve is the Craigie parameterization. The PHENIX point at $y = 0$ is included.

$b\bar{b}$ Data Fixes Mass and Scale for CEM Bottomonium Calculations

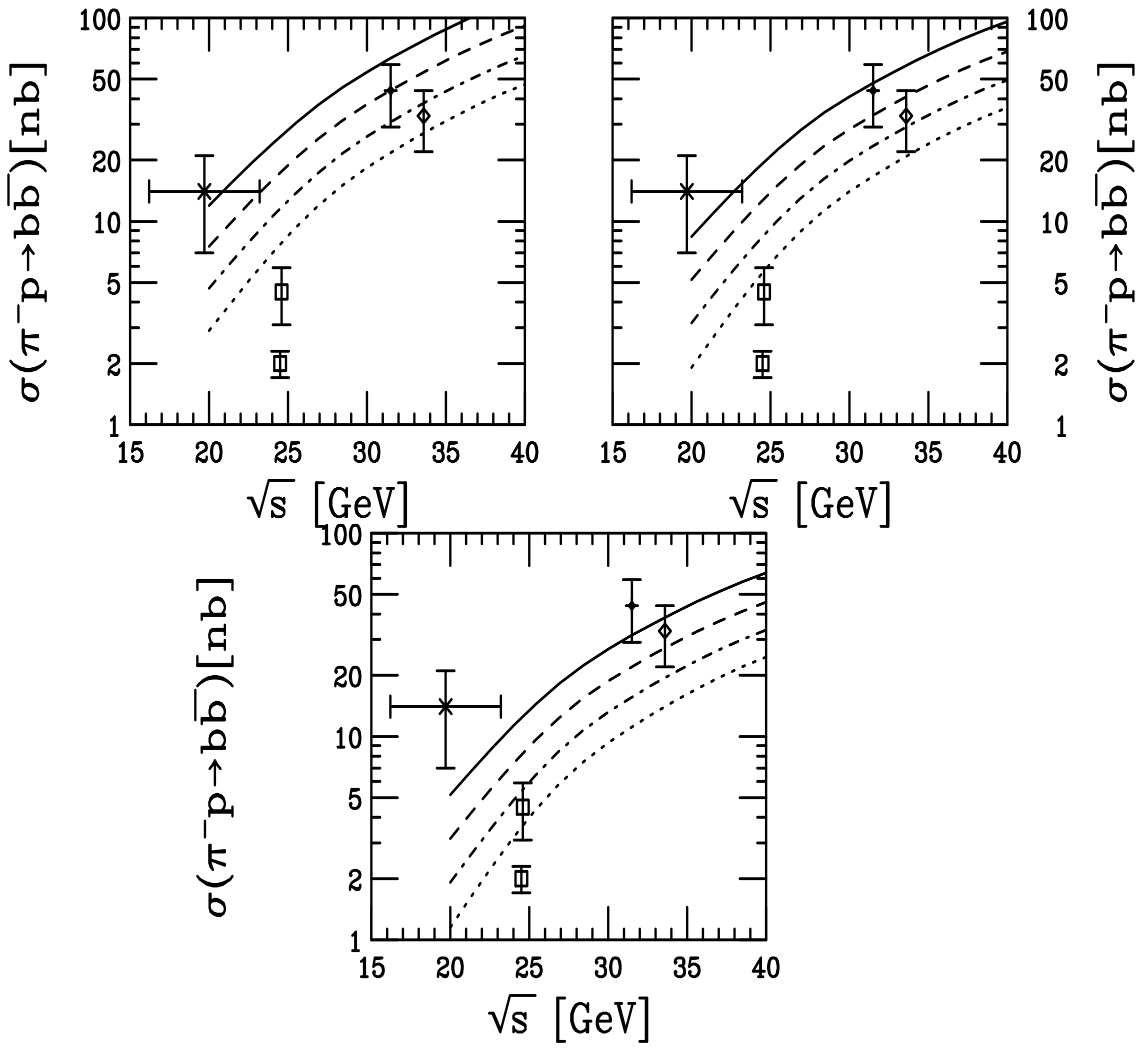

Figure 12: Total $b\bar{b}$ cross sections in $\pi^- p$ interactions as a function of m_b. These NLO calculations use the MRST HO parton densities. From the upper left, the plots show results with $\mu = m_b/2$, m_b and $2m_b$ respectively. In each plot, from top to bottom the curves are $m_b = 4.25$, 4.5, 4.75, and 5 GeV.

Parameters From $b\overline{b}$ Cross Sections

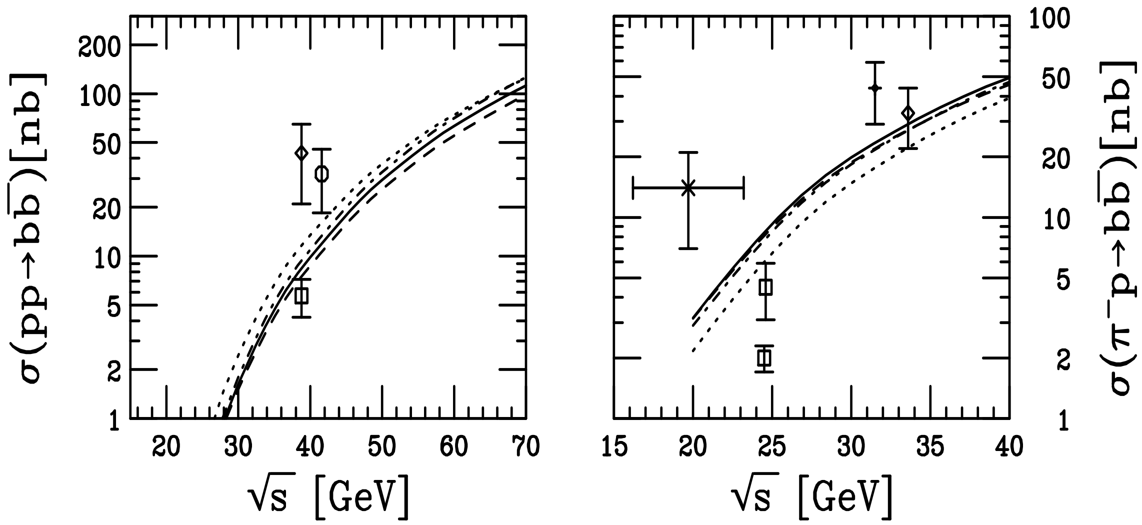

Figure 13: Total $b\overline{b}$ cross sections in pp and $\pi^- p$ interactions. The curves are: MRST HO with $\mu = m = 4.75$ GeV (solid), $\mu = 2m = 9$ GeV (dashed), and $\mu = m/2 = 2.5$ GeV (dot-dashed); GRV 98 HO with $\mu = m = 4.75$ GeV.

Case	PDF	m_b (GeV)	μ/m_b	$\sigma_{B\sum\Upsilon}/\sigma_b^{\rm CEM}$	$\sigma_\Upsilon/\sigma_b^{\rm CEM}$
Υ1	MRST HO	4.75	1	0.000963	0.0276
Υ2	MRST HO	4.50	2	0.000701	0.0201
Υ3	MRST HO	5.00	0.5	0.001766	0.0508
Υ4	GRV 98 HO	4.75	1	0.000787	0.0225

Table 3: The production fractions obtained from fitting the CEM cross section to the combined Υ cross sections to muon pairs at $y = 0$ as a function of energy. The PDF, charm quark mass, and scales used are the same as those obtained by comparison of the $b\overline{b}$ cross section to the $\pi^- p$ data.

Inclusive Υ Cross Sections at $y = 0$

Cross sections include all $\Upsilon(nS)$ states and their decays to muon pairs

Data is from pp interactions except for highest two points where only $p\overline{p}$ colliders available

At high energies, $gg \to Q\overline{Q}$ dominates and differences between $p\overline{p} \to \Upsilon$ and $pp \to \Upsilon$ are negliglble

LHC ion energy only a factor of 3 beyond Tevatron Run I

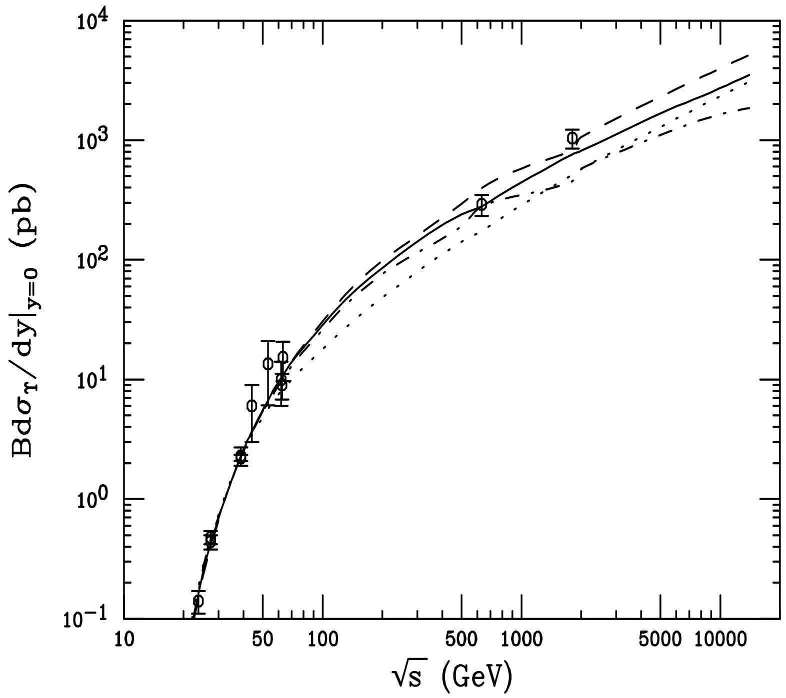

Figure 14: Inclusive Υ production data, combined from all three S states, and compared to NLO CEM calculations. The solid curve employs the MRST HO distributions with $m_b = \mu = 4.75$ GeV, the dashed, $m_b = \mu/2 = 4.5$ GeV, the dot-dashed, $m_b = 2\mu = 5$ GeV, and the dotted, GRV 98 HO with $m_b = \mu = 4.75$ GeV.

Comparison to CDF Bottomonium Data

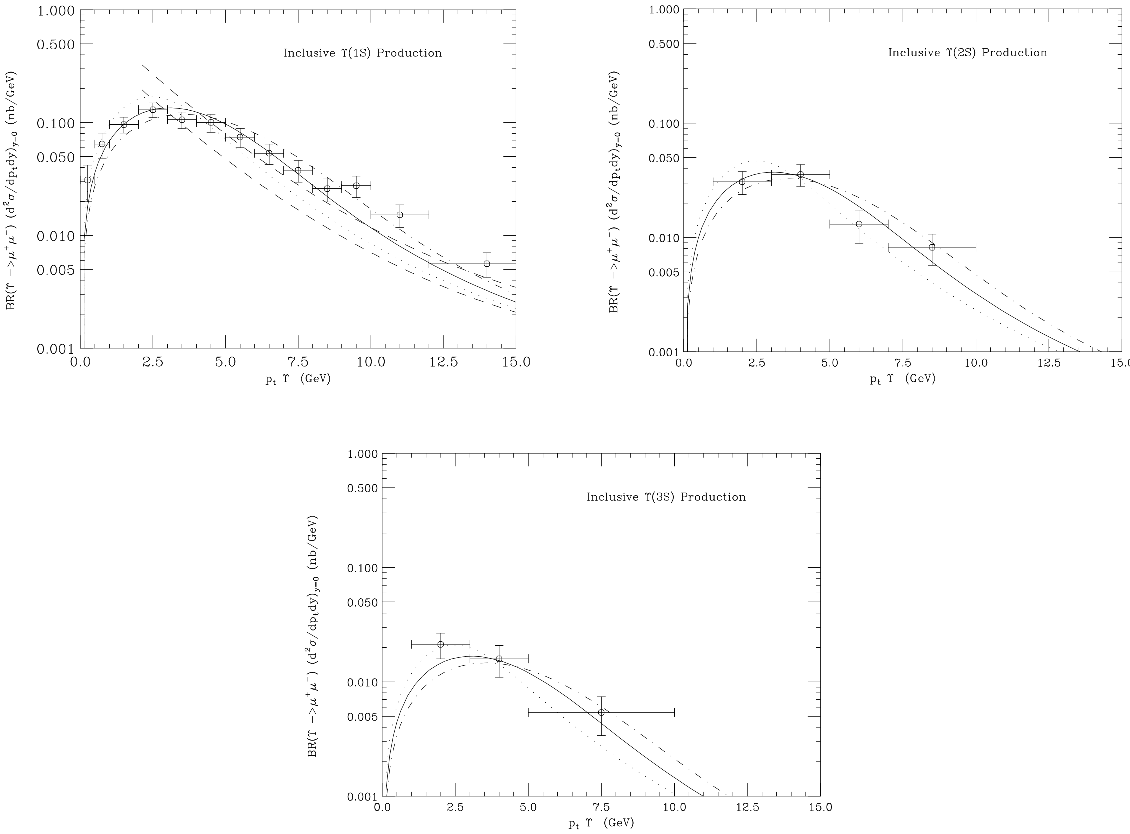

Figure 15: Transverse momentum distributions of bottomonia compared to CDF data for various values of the intrinsic transverse momentum: $\langle k_T \rangle = 1.25\,\mathrm{GeV}$ (dotted), $2.0\,\mathrm{GeV}$ (solid), $2.5\,\mathrm{GeV}$ (dot-dashed). The $\Upsilon(1S)$ prediction without smearing, $\langle k_T \rangle = 0$, is shown as dashed lines. The upper dashed curve without smearing contains a K factor of 1.9. From G. Schuler and R.V., Phys. Lett. **B387** (1996) 181.

Summary

- Color Evaporation Model makes no great claims—only that ratios of quarkonium cross section remain constant as a function of kinematics
- Then parameters fit at one energy should apply to all energies
- Color evaporation hadroproduction results are in relatively good agreement with the entire energy range measured so far